Efficiency evaluation of a natural material for removal of cationic oxazine and anionic azo dyes from aqueous solutions

Asma Boudaoud[1], Chifaa Ad[2], Mebrouk Djedid[2], Mokhtar Benalia[2], Mounira Guermit[1] and Soltani Amel[3]

[1]Laboratory of Process Engineering, Materials and Environmental, Department of Common Trunk Science and Technology; Faculty of Technology, Amar Telidji University of Laghouat, Laghouat, Algeria
[2]Laboratory of Process Engineering, Materials and Environmental, Department of Process Engineering, Faculty of Technology, Amar Telidji University of Laghouat, Laghouat, Algeria
[3]Higher Normal School of Laghouat, Laghouat, Algeria

Abstract

The current work involves studying the adsorption process of brilliant cresyl blue (BCB) and methyl orange (MeO) dyes using local pumpkin seed husks (LPSH). The LPSH adsorbent was analysed by using Fourier transform infrared spectroscopy, scanning electron microscopy with energy dispersive x-ray spectroscopy, X-ray diffraction and Brunauer-Emmett-Teller analyses. The descriptive analysis of the morphology of LPSH revealed a heterogeneous surface, while the structural analysis showed the presence of functional groups typical of lignocellulosic structures and it was confirmed that the mesoporous surface of the adsorbent had a specific surface area of ~1.53 $m^2 g^{-1}$. The adsorption isotherm studies suggested that the Langmuir model best described the adsorption of MeO, while the Freundlich model is more suitable for describing the adsorption of BCB. According to the thermodynamic analyses, the adsorption of BCB was exothermic and spontaneous, whereas the adsorption of MeO was endothermic and non-spontaneous. The results of evaluating the efficiency of the LPSH adsorbent showed that the maximum adsorption capacities are ~81 mg g^{-1} for the BCB dye and ~8.2 mg g^{-1} for the MeO dye.

Keywords: Brilliant cresyl blue; methyl orange; adsorption; pumpkin seed husks; synthetic dye solutions.

Available on-line at the Journal web address: http://www.ache.org.rs/HI/

TECHNICAL PAPER

UDC: 547.556.33-045.38

Hem. Ind. **00(0)** 000-000 (2025)

1. INTRODUCTION

Water quality can be compromised due to the presence of harmful substances originating from various sources, such as industrial discharges, agricultural runoff, and sewage. The resulting pollution can be classified based on the type of pollutants: chemical, biological, or physical, along with the source and the amount of water affected. To understand how polluted the water is, it is necessary to determine concentrations of the contaminants and how they impact different uses of the water (*e.g.* for drinking), as well as aquatic life, and recreational activities [1]. Also the pollutants can be divided into several categories, such as natural and synthetic pollutants [2-4].

Synthetic dyes such as Brilliant cresyl blue and methyl orange are compounds used in many industrial sectors such as the paper industry, printing, natural and synthetic textiles production, leather and fur industry, plastics manufacturing, and pharmaceutical industry, as well as in research laboratories [5,6]. These dyes are discharged with liquid effluents into streams without prior treatment. High toxicity of these pollutants and their non-biodegradability contribute to environmental degradation [7] imposing the need for treatment of this wastewater.

Work on the removal of emerging pollutants by biomaterials obtained from agricultural waste has yielded promising results. Thus, these precursors from agriculture constitute alternative materials, both economic and eco-friendly [8-10]. In addition, enormous amounts of waste are generally available from farms and agro-industrial facilities in many countries, where agricultural residues notably represent a significant unused resource.

Corresponding author: Asma Boudaoud, Amar Telidji University of Laghouat, Laghouat, Algeria
E-mail: a.boudaoud@lagh-univ.dz
Paper received: 26 November 2023; Paper accepted: 27 March 2025; Paper published: 1 Mayl 2025.
https://doi.org/10.2298/HEMIND231126006B

This research aims to evaluate local pumpkin seed husks (LPSH) as a naturally adsorbing material for removing cationic dye brilliant cresyl blue and anionic dye methyl orange from synthetic wastewater by a batch adsorption process.

For this purpose, this study includes the examination of raw LPSH characteristics using Fourier transform infrared spectroscopy (FTIR), scanning electron microscopy with energy dispersive X-ray spectroscopy (SEM-EDX), X-ray diffraction (XRD), and Brunauer-Emmett-Teller (BET) and Barrett-Joyner-Halenda (BJH) methods. Also, effects of various operational variables have been studied such as pH value of the solution, contact time, initial concentration, and temperature. This work also includes investigations of the most significant isotherm models, as well as thermodynamic parameters, to accurately define the mechanism and behaviour of the dye adsorption.

1. MATERIALS AND METHODS

2. 1. Materials

Chemical reagents used in this study were cationic oxazine dye Brilliant cresyl blue (BCB: $C_{34}H_{40}Cl_4N_6O_2Zn$, purity >95 %), anionic azo dye: methyl orange (MeO: $C_{14}H_{14}N_3NaO_3S$, purity >98 %), sodium hydroxide (NaOH, purity > 80% and sulfuric acid (H_2SO_4, purity >95 %), all obtained from Fluka and Sigma-Aldrich (Germany).

2. 2. Preparation of pumpkin seed husks

Local pumpkin seed husks (*Cucurbita moschata*) from Laghouat, Algeria, were selected as the adsorbent for this investigation. It was prepared by using a simple method that involved washing with distilled water, grinding, sifting, and drying for 24 h at 105 ± 5 °C. A fine pumpkin seed husks powder with a particle size of ≤ 800 μm was obtained as a result of this method [11].

2. 3. Characterization of pumpkin seed husks

Structural and morphological characteristics of LPSH samples have been evaluated using the Fourier transfer infrared (FTIR) spectroscopy (4200-FTIR JASCO, Japan), scanning electron microscopy combined with energy dispersive X-ray (SEM-EDX, Thermo Scientific™ Quattro, United States), and X-ray diffraction (XRD, Philips PW3373, United Kingdom). Specific surface area and porosity parameters were determined by using the Brunauer-Emmett-Teller (BET) and Barrett-Joyner-Halenda (BJH) methods (ASAP 2020 Plus Version 2.00–Malvern Panalytical, Malvern, United States). One sample was prepared for each test.

2. 4. Preparation of dye solutions

Dyes used in this study were BCB and MeO (Fig. 1), with the chemical formula: $C_{34}H_{40}Cl_4N_6O_2Zn$ and $C_{14}H_{14}N_3NaO_3S$, respectively. The dyes were dissolved so to prepare the stock solutions of 1000 mg dm^{-3}, (2.6 and 3.1 mmol dm^{-3}, respectively) and different concentrations were obtained by diluting the stock solutions. To change the pH of the dye solutions, either 0.1 mol dm^{-3} NaOH or 0.2 mol dm^{-3} H_2SO_4 solutions were added.

2. 5. Batch adsorption experiments

Adsorption experiments were carried out in batch mode in 150 cm^3 beakers placed on a shaker at 150 rpm. In each beaker, a dose of LPSH was carefully mixed with 100 ± 1.0 cm^3 of BCB or MeO solutions for studying the influence of factors such as the adsorbent dose, pH, contact time, initial concentration and temperature. A series of batch adsorption experiments were conducted with factors modified according to the One-Factor-at-a-Time (OFAT) method [12]. The experiments involved different conditions, as shown in Table 1.

All dye samples were filtered and diluted to measure the dye concentrations before, after, and at equilibrium adsorption using an UV-Visible spectrophotometer (UVILINE 9400, France) at maximum wavelengths: λ_{max}=627 nm for BCB and λ_{max}=465 nm for MeO at pH≥4, λ_{max}=508 nm for MeO at pH <4 (Fig. 1). The experiments were repeated and measured three times for accuracy.

Table 1. *Experimental conditions for investigating the effects of different adsorption factors*

Experiment	Factor	Conditions
1	Adsorbent mass: 0 to 1 g	Initial concentration = 15 mg dm^{-3} (39 μmol dm^{-3} for BCB and 46 μmol dm^{-3} for MeO) pH 3.7 for BCB and pH 6.62 for MeO Contact time = 180 min Temperature = 298 K
2	pH solution: 2 to 8	Initial concentration = 15 mg dm^{-3} (39 μmol dm^{-3} for BCB and 46 μmol dm^{-3} for MeO) Adsorbent mass = 0.1 g for BCB and 0.2 g for MeO Contact time = 180 min Temperature = 298 K
3	Contact time: 0-180 min	Initial concentration = 50 mg dm^{-3} (130 μmol dm^{-3} for BCB and 153 μmol dm^{-3} for MeO) pH = 5 for BCB and pH=7 for MeO Adsorbent mass = 0.1 g for BCB and 0.2 g for MeO Temperature = 298 K
4	Initial concentration: 15 to 100 mg dm^{-3} (39 to 259 μmol dm^{-3} for BCB; 46 to 305.5 μmol dm^{-3} for MeO)	Adsorbent mass = 0.1 g for BCB and 0.2 g for MeO pH 5 for BCB and pH 7 for MeO Contact time = 20 min for BCB and 90 min for MeO Temperature = 298 K
5	Temperature: 298-328 K	Initial concentration = 50 mg dm^{-3} (130 μmol dm^{-3} for BCB and 153 μmol dm^{-3} for MeO) pH 5 for BCB and pH 7 for MeO Contact time = 20 min for BCB and 90 min for MeO Adsorbent mass = 0.1 g for BCB and 0.2 g for MeO

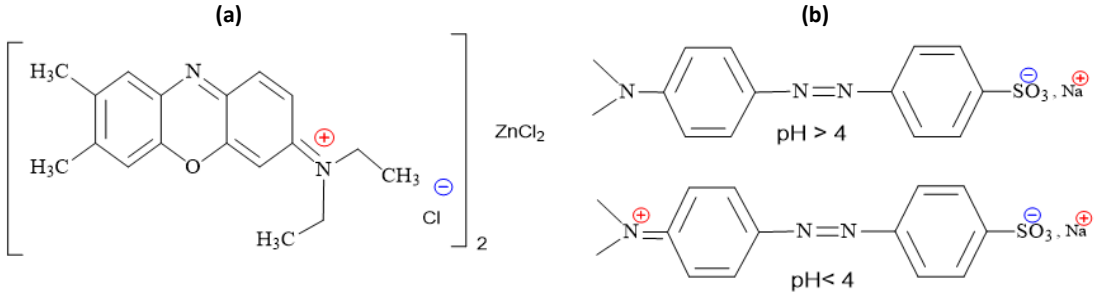

Figure 1. *Chemical structures of (a) - brilliant cresyl blue and (b) - methyl orange*

In order to quantify the adsorption performance of LPSH for BCB and MeO, the amounts of dyes adsorbed per unit mass of LPSH, *Q*, were calculated using the following equation:

$$Q = \frac{(C_i - C_t)V}{W} \quad (1)$$

where C_i and C_t are the initial and concentration at time *t*, respectively, *V* is the volume of dye solution, and *W* is the weight of the LPSH adsorbent.

2. RESULTS AND DISCUSSION

3. 1. Adsorbent characterization

Infrared spectroscopy analyses (FTIR) were performed to determine functional groups characterizing this LPSH adsorbent (Figure 2).

The spectrum shows a large band at 3432.71 cm^{-1}, which is attributed to the stretching vibration of O-H hydroxyl groups or amine groups (N–H). While aliphatic C-H stretching vibrations are characterized by a band between 2907.19 and 2843.15 cm^{-1}. It was determined, from the LPSH spectrum, that the carbonyl (C=O) stretch at 1735.37 cm^{-1} indicates the presence of a carbonyl-containing functional group (carboxylic acid, ketone, aldehyde, or lactone). The asymmetric stretch of a carboxylate (COO^-) group is indicated by the band at 1592.34 cm^{-1}. The aromatic C=C stretching vibrations are characterized by two additional bands at 1424.59 and 1377.26 cm^{-1}. The band at 1034.10 cm^{-1} was assigned to C-O-C ether groups. The results obtained by this spectrum are similar to those observed for other lignocellulosic materials [13,14].

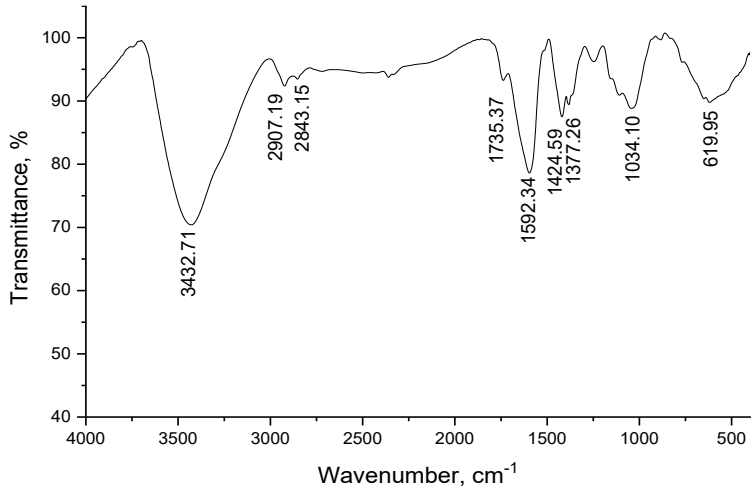

Figure 2. *FTIR spectrum of pumpkin seed husks*

Morphology analysis and elemental identification were performed by using an SEM-EDX device, providing the results reported in Figure 3 and Table 2. The results show that LPSH has a heterogeneous and rough surface, which contains few holes and cavities. Elemental identification at the EDX spectrum confirmed that the adsorbent LPSH consists of molecules containing carbon (C) and oxygen (O) with major weight of 51.85 % for C (with a specific measurement repetition of 0.9405) and 48.15 % for O (with a specific measurement repetition of 0.9495).

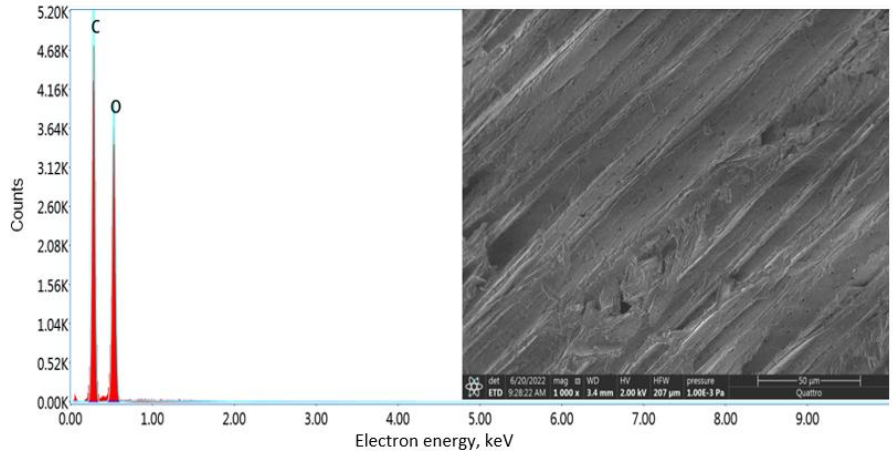

Figure 3. *SEM micrograph and EDX spectrum of pumpkin seed husks*

Table 2. *Elemental identification of pumpkin seed husks by the EDX analysis*

Element	Content, wt.%	Content, at.%	Error, %	Net Intensity
C K	51.85	58.92	7.51	522.93
O K	48.15	41.08	8.90	427.88

According to the X-ray analysis of an LPSH sample shown in Figure 4, there are three peaks at 2θ angles of 16.07, 22.34 and 34.30°. The presence of distinct peaks at 22.34 and 34.30° indicates semi-crystalline regions, while the broader feature around 16.07° suggests an amorphous component structures of pumpkin seed husks. This structure typically distinguishes agricultural materials , consisting of cellulose, lignin, and hemicellulose [15,16].

BET and BJH methods were used to quantify the surface area and porosity of a LPSH sample by studying nitrogen adsorption and desorption isotherms. The results shown in Figure 5 indicate that the obtained N_2 isotherm is classified as type IV (H3) according to the IUPAC classification, signifying a mesoporous material with slit-shaped pores in plate-like aggregates, showing multilayer adsorption, capillary condensation and complex pore connectivity [17]. The BET surface area was measured as 1.5300 ± 0.0272 $m^2\ g^{-1}$, with a total pore volume of 0.0014 $cm^3\ g^{-1}$ and an average pore diameter of 3.70 nm. Furthermore, the pore size in the range of 2 to 50 nm corresponds to mesoporous materials [18].

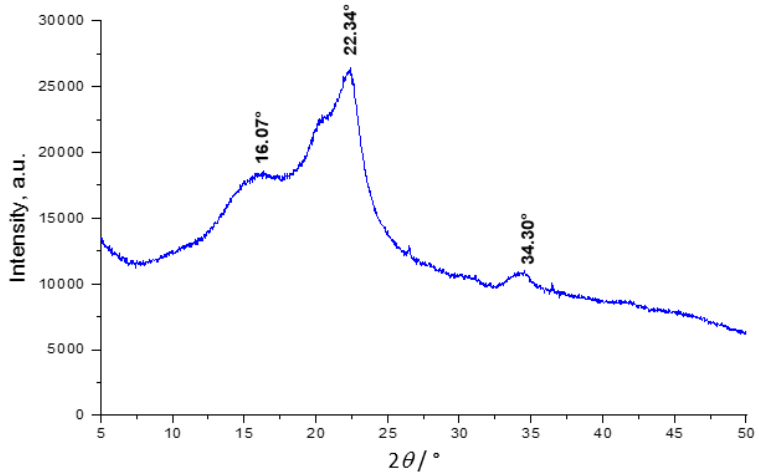

Figure 4. *X-ray diffraction analysis of pumpkin seed husks*

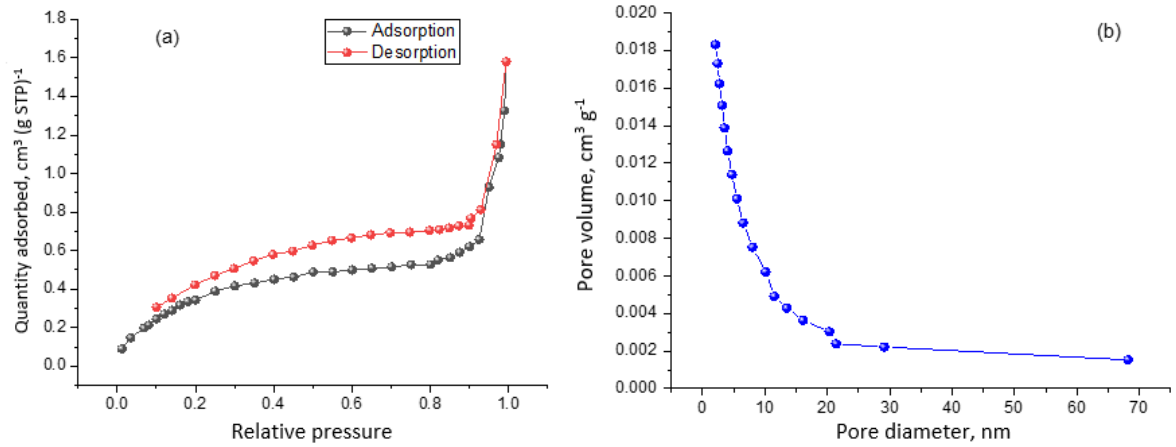

Figure 5. *BET analysis of N_2 adsorption-desorption isotherm (a) and pore size distribution of LPSH (b)*

3. 2. Effect of physico-chemical parameters

3. 2. 1. Effect of pH

The pH of a dye solution is important factor in any adsorption study, as it affects the charge of the adsorbent's surface and the behaviour of the adsorbed ions [19]. The result of this test is illustrated in Figure 6(a). Due to electrostatic interactions between the anionic dye MeO and the positive sites of LPSH, MeO dye is adsorbed most effectively at pH 7 [20].

In the case of the cationic dye (BCB), adsorption increases by rising the pH, indicating less competition for negative sites on the surface of the adsorbent, reaching its maximum at pH 5.

3. 2. 2. Effect of contact time

Generally, increasing contact time results in an increase in the adsorbed amount until reaching the equilibrium, as was also obtained in the present study (Fig. 6(b)). The BCB adsorption reaches equilibrium after 20 min, while for dye MeO the equilibrium is reached after 90 min. This difference is attributed to the higher number of active sites available on the adsorbent surface for the BCB dye as compared to those available for dye MeO the initial dye concentrations were 130 and 153 μmol/md^{-3} for BCB and MeO, respectively, while the equilibrium adsorbed amounts were 209 and 25 μmol/g, for BCB and MeO. A similar pattern of behaviour for the adsorption of dyes BCB and MeO was observed in other related research [21,22].

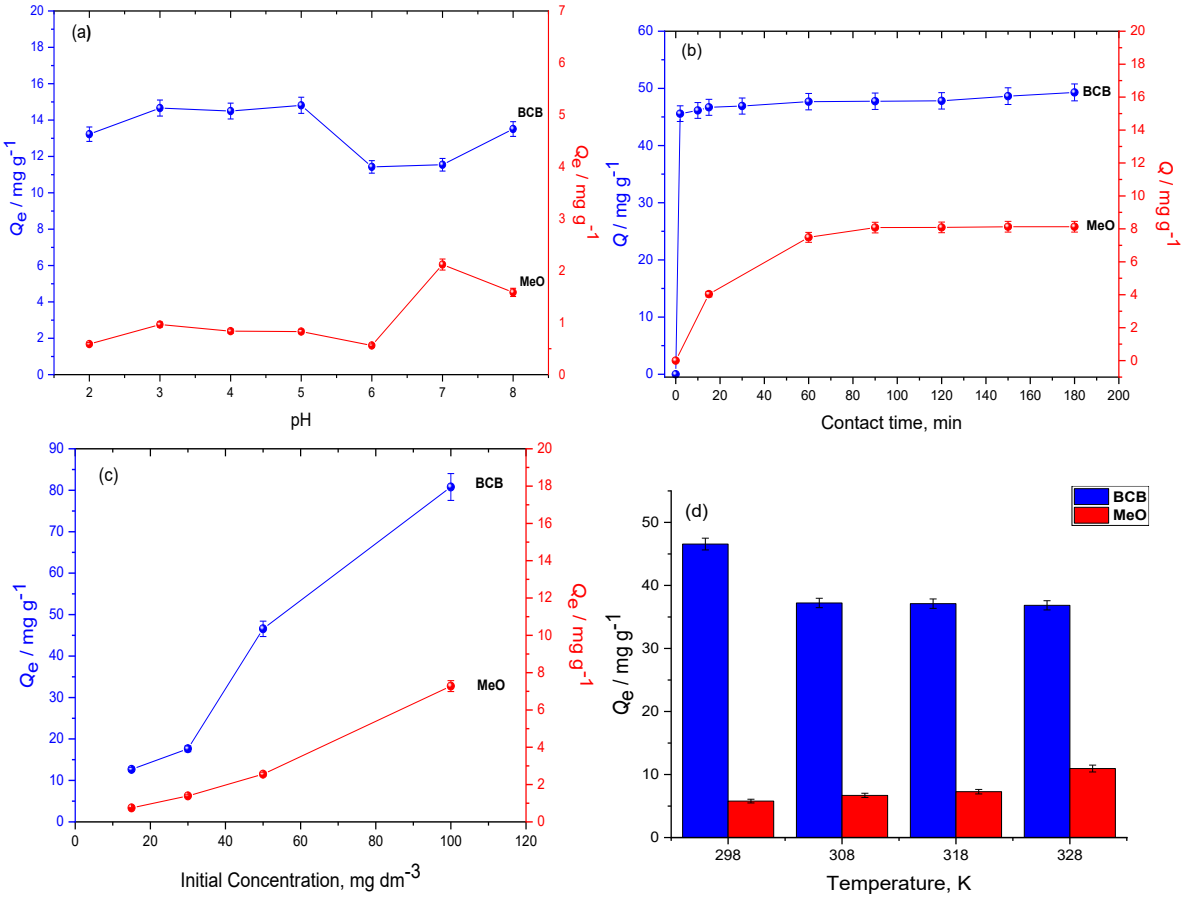

Figure 6. *Adsorption of BCB and MeO onto LPSH: (a) - equilibrium adsorbed dye amount per the adsorbent mass (Q_e) as a function of the solution pH, (b) - adsorbed dye amount per Q as a function of the contact time, (c) - equilibrium adsorbed dye amount per Q_e as a function of the initial dye concentration, (d) - equilibrium adsorbed dye amount per Q_e as a function of the temperature; all experimental conditions for each experimental series are provided in Table 1*

3. 2. 3. Effect of initial concentration

As shown in Figure 6(c), the increase in adsorbed amounts is observed with an increase in the initial concentrations of BCB and MeO, as expected. However, it can be concluded that both dyes do not occupy all the active sites of the adsorbent.

3. 2. 4. Effect of temperature

The influence of temperature on the adsorption of MeO and BCB was studied in the range 298 to 328 K (Fig. 6(d)). It can be noted that that as the temperature rises, the amount of BCB that can be adsorbed decreases slightly (indicating an inverse relationship). This can be explained by the weakening of the bonds between BCB and the active sites of the adsorbent. The results suggest that the adsorption of BCB by LPSH adsorbent is exothermic. In contrast, in the case of MeO, the adsorbed amount increases with rising the temperature. This is because the mobility of MeO molecules increases at higher temperatures, enhancing the interaction between MeO and the active sites of the adsorbent LPSH. The obtained result indicate that adsorption of MeO by LPSH is an endothermic process [23].

3. 3. Adsorption isotherm studies

Adsorption is governed by mathematical equations that relate the adsorbed amount to the equilibrium concentration of the solute. Thus, the adsorbed amount (per unit adsorbent mass) plotted as a function of the equilibrium concentration at constant temperature represents the adsorption isotherm. Among the most commonly used isothermal models are the Freundlich [24] and Langmuir [25] isotherms.

The results obtained allowed for the plotting of linear shapes according to the Freundlich (Equation (2)) and the Langmuir (Equation (3)) isothermal models (Figure 7), enabling calculation of the various constants for both models.

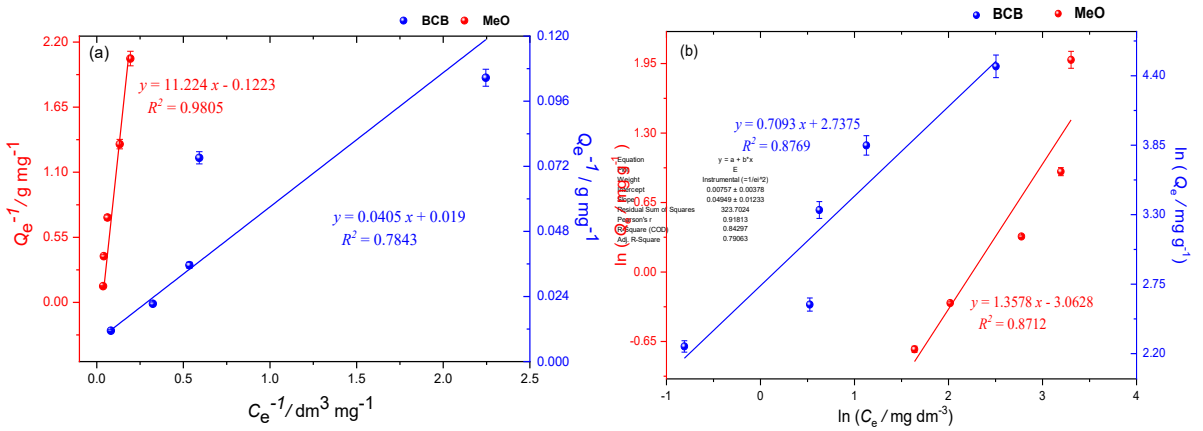

Figure 7. *Linear fits of Langmuir (a) and Freundlich (b) isotherms and equilibrium data for BCB and MeO adsorption onto LPSH, experimental conditions: initial dye concentrations C_0: 15 to 100 mg dm^{-3}(39 μmol dm^{-3} for BCB and 46 μmol dm^{-3} for MeO); W = 0.1 g for BCB and 0.2 g for MeO; pH 5 for BCB and pH 7 for MeO; contact time 20 min for BCB and 90 min for MeO; T = 298 K*

$$\ln Q_e = 1/n \ln C_e + \ln K_F \quad (2)$$

$$1/Q_e = 1/Q_m + 1/K_L Q_m \, 1/C_e \quad (3)$$

where Q_m / mg g^{-1} is the maximum adsorption capacity of a saturated monolayer onto the adsorbent's surface; K_L / dm^3 mg^{-1} is the rate constant of the Langmuir model; K_F / mg^{1-n} dm^{3n} g^{-1} is the Freundlich constant of the maximum adsorption capacity and n is the empirical constant related to the adsorbent surface heterogeneity.

The calculated constants of the Freundlich and Langmuir models show that the Freundlich isotherm was best adapted to the experimental results, with a correlation coefficient R^2 of 0.8769, with a maximum experimental BCB adsorption of 80.7± 4.0 mg g^{-1} (209 ± 10 μmol g^{-1}) indicating the possibility of multilayer adsorption of BCB onto LPSH [26]. For MeO adsorption the results obtained show that the Langmuir isotherm provided the best fit to the experimental data, with a correlation coefficient R^2 of 0.9805, and the calculated maximum adsorption capacity of MeO was 8.2 ± 0.0 mg g^{-1} (25 ± 0 μmol g^{-1}), suggesting a homogeneous monolayer arrangement of MeO dye on the LPSH surface [27].

3. 4. Thermodynamic studies

Thermodynamic parameters such as the enthalpy change (ΔH°), entropy change (ΔS°) and free energy change (ΔG°) are essential for a better understanding of the temperature effects on the energies of adsorption.

The values of ΔH° and ΔS° were estimated from the graphical presentation of ΔG° as a function of temperature T according to Equations (4), (5) and (6) [28]:

$$K_d = \frac{Q_e}{C_e} \quad (4)$$

$$\Delta G° = -RT \ln K_d \quad (5)$$

$$\Delta G° = \Delta H° - T\Delta S° \quad (6)$$

where R is the ideal gas constant, 8.314 J mol^{-1}·K^{-1}; T / K is temperature and K_d is the distribution constant.

Figure 8 shows the evaluation of thermodynamic parameters with respect to temperature of BCB and MeO adsorption onto pumpkin seed husks. From the obtained curves, which include the thermodynamic parameters for BCB and MeO adsorption, we observe that ΔG° as a function of temperature is linear, and its negative values (-6.46 to -1.98 kJ mol^{-1}) indicate the spontaneous adsorption of BCB, while the adsorption of MeO is non-spontaneous process (ΔG°= 4.92 to 2.87 kJ mol^{-1}) [16]. Moreover, the positive values of ΔH° (+25.01 ± 1.17 kJ mol^{-1}) suggest endothermic process of MeO and the negative values of ΔS° (-67.64 ± 3.74 J mol^{-1} K^{-1}) indicate an increasing order at the interface LPSH/MeO during this adsorption. In contrast, the adsorption of BCB onto LPSH is an exothermic process (ΔH°=-45.31 ± 17.72 kJ mol^{-1} < 0) [29], with an increase in randomness between the BCB dye and the LPSH adsorbent (ΔS°= +133.60 ± 56.59 J mol^{-1} K^{-1} > 0) [30].

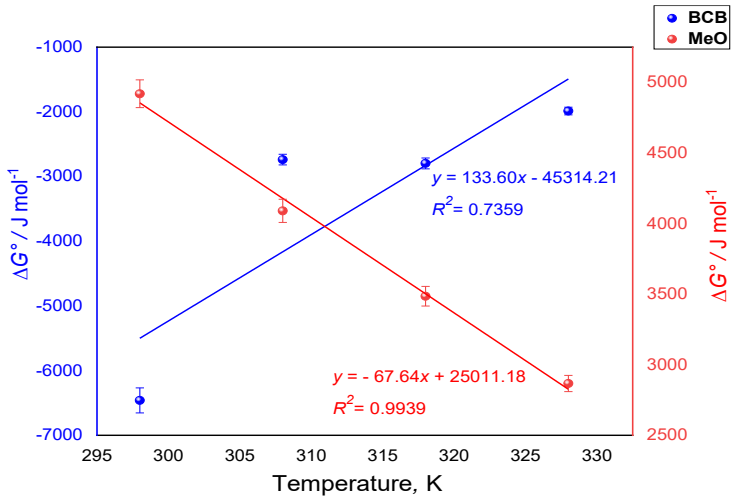

Figure 8. *Linear plots of free energy versus temperature, experimental conditions: C_0: 50 mg dm^{-3} (130 μmol dm^{-3} for BCB and 153 μmol dm^{-3} for MeO); W = 0.1 g for BCB and 0.2 g for MeO; pH 5 for BCB and pH 7 for MeO; contact time = 20 min for BCB and 90 min for MeO; T = 298 to 328 K; shaker speed = 150 rpm.*

3. 5. Comparative studies

The pumpkin seed husk adsorbent used in the present study exhibited superior BCB dye adsorption compared to previous studies using raw, unmodified agricultural residues (Table 3), achieving high removal efficiency in a significantly shorter time-frame, while the results for dye MeO adsorption were acceptable.

Table 3. *Comparative evaluation of agricultural waste materials as adsorbents for BCB and MeO dyes*

Adsorbents	Adsorbates	Isotherm model	Adsorption capacity, mg g^{-1}	Ref.
Inula Racemosa leaves	BCB	Freundlich	3.49 at 10 min	[31]
Peanut hull			4.39 at 12 h	[32]
Pumpkin seed husks			80.7 at 20 min	Present work
Anchote peel	MeO		103.03 at 140 min	[33]
Palm fibers		Langmuir	48.79 at 120 min	[34]
Sawdust			50.52 at 120 min	[34]
Pumpkin seed husks			8.2 at 90 min	Present work

4. CONCLUSION

With the aim of evaluating the efficiency of Algerian pumpkin seed husks in removing cationic and anionic dye pollutants, this research has focused first on studying the characteristics of the surface of this adsorbent. The results indicate that the surface of the seed husks is not homogeneous; it is rough and consists of mesopores, with a significant specific surface area of 1.53 ± 0.027 m^2 g^{-1} and is rich in organic chemical groups responsible for the fixation of BCB and MeO dyes through electrostatic attraction and hydrogen bonds.

The results obtained in the adsorption studies allowed us to advance the following points:

Isothermal study: the adsorption of BCB dye was well described by the Freundlich isotherm, with a maximum adsorption capacity of 80.7± 4.038 mg g^{-1} (209 ± 10 μmol g^{-1}). In contrast, the Langmuir isotherm was more favorable for the adsorption of MeO dye onto LPSH, with a maximum adsorption capacity of 8.2 ± 0.004 mg g^{-1} (25 ± 0 μmol g^{-1}).

Thermodynamic study: the results show that the adsorption process for BCB dye using the LPSH adsorbent was spontaneous and exothermic, while the adsorption process for MeO dye was non-spontaneous and endothermic.

Overall, the results of our work indicate that this study is significant in demonstrating that raw LPSH has an acceptable and favorable adsorption capacity compared to other adsorbents.

Acknowledgement: The authors gratefully acknowledge the support and accompaniment of the Directorate General of Scientific Research and Technological Development Algeria and the Algerian Ministry of Higher Education and Scientific Research.

REFERENCES

[1] Chaudhry FN, Malik MF. Factors Affecting Water Pollution. *A Rev J Ecosyst Ecography.* 2017; 7(225): 1-3. https://doi.org/10.4172/2157-7625.1000225

[2] Hussain S, Khan N, Gul S, Khan S, Khan H. *Contamination of Water Resources by Food Dyes and Its Removal Technologies.* In Water Chemistry. *Eds; Intech Open London, UK,* 2020. https://doi.org/10.5772/intechopen.90331

[3] Iwuozor KO, Ighalo JO, Emenike EC, Ogunfowora LA, Igwegbe CA. Adsorption of methyl orange: A review on adsorbent performance. *Curr Res Green Sustain Chem.* 2021; 4: 100179. https://doi.org/10.1016/j.crgsc.2021.100179

[4] Al-Gubury HY, Alteemi HS, Saad AM , Al-Shamary RR. Removal of Hazardous Brilliant Cresyl Blue Dye Utilizing Aluminum Oxide as Photocatalyst. *Indones J Chem.* 2019; 19(2): 292-297. https://doi.org/10.22146/ijc.30135

[5] Alhujaily A., Yu H., Zhang X. Ma F. Adsorptive removal of anionic dyes from aqueous solutions using spent mushroom waste. *Appl Water Sci.* 2020; 10: 183. https://doi.org/10.1007/s13201-020-01268-2

[6] Cako E, Gunasekaran KD, Soltani RDC, Boczkaj G. Ultrafast degradation of brilliant cresyl blue under hydrodynamic cavitation based advanced oxidation processes (AOPs). *Water Resour Ind.* 2020; 24: 100179. https://doi.org/10.1016/j.wri.2020.100134

[7] Adegoke KA, Bello OS. Dye sequestration using agricultural wastes as adsorbents. *Water Resour Ind.* 2015; 12: 8-24. https://doi.org/10.1016/j.wri.2015.09.002

[8] Zulti F, Setiadewi N, Waluyo A, & Susanti E. Removal pollutants in textile wastewater using unmodified rice husk. *E3S Web Conf.* 2024; 483: 02008. https://doi.org/10.1051/e3sconf/202448302008

[9] Yetgin S, Amlani M. Agricultural low-cost waste adsorption of methylene blue and modelling linear isotherm method versus nonlinear prediction. *Clean Technol Environ Policy*. 2024. https://doi.org/10.1007/s10098-024-02928-6

[10] Alivio RKO, Go AW, Angkawijaya AE, Santoso SP, Gunarto C, Soetaredjo FE. Extractives-free sugarcane bagasse as adsorbent for the removal of Rhodamine B (Basic Violet 10) with high capacity and reusability. *J Ind Eng Chem*. 2023; 124: 175-200. https://doi.org/10.1016/j.jiec.2023.04.007

[11] Ad C, Benalia M, Laidani Y, Elmsellem H, Henini G, Nouacer I, Djedid M. Kinetics, thermodynamics and equilibrium evaluation of adsorptive removal of iron from aqueous solution onto Algerian biosorbent "LUFFA CYLINDRICA." *J Mater Environ Sci.* 2016; 7(1): 319-30. https://www.jmaterenvironsci.com/Document/vol7/vol7_N1/34-JMES-1968-2012-Ad.pdf

[12] Frey DD, Wang H. Adaptive One-Factor-at-a-Time Experimentation and Expected Value of Improvement. *Technometrics*. 2006; 48(3): 418-431. https://doi.org/10.1198/004017006000000075

[13] Awoyale AA, Lokhat D. Experimental determination of the effects of pretreatment on selected Nigerian lignocellulosic biomass in bioethanol production. *Sci Rep.* 2020; 11: 557. https://doi.org/10.1038/s41598-020-78105-8

[14] Khalfaoui A, Khelifi MN, Khelfaoui A, Benalia A, Derbal K, Gisonni C, Crispino G, Panico A A. The Adsorptive Removal of Bengal Rose by Artichoke Leaves: Optimization by Full Factorials Design. *Water.* 2022; 14(14): 2251. https://doi.org/10.3390/w14142251

[15] Ishak WHW, Ahmad I, Ramli S, Amin MCIM. Gamma Irradiation-Assisted Synthesis of Cellulose Nanocrystal-Reinforced Gelatin Hydrogels. *Nanomaterials.* 2018; 8: 749. https://doi.org/10.3390/nano8100749

[16] Kali A, Amar A, Loulidi I, Hadey C, Jabri M, Alrashdi AA, Lgaz H, Sadoq M. Efficient Adsorption Removal of an Anionic Azo Dye by Lignocellulosic Waste Material and Sludge Recycling into Combustible Briquettes. *Colloids Interfaces.* 2022; 6: 22. https://doi.org/10.3390/colloids6020022

[17] Purbasari A, Ariyanti D, Sumardiono S, Masyaroh M, Salsabila TR. Physical properties and structural characteristics of alkali modified fly ash. *J Phys Conf Ser.* 2021; 1912: 012012. https://doi.org/10.1088/1742-6596/1912/1/012012

[18] Horvat G, Pantic M, Knez Z, Novak Z. A Brief Evaluation of Pore Structure Determination for Bioaerogels. *Gels.* 2022; 8(7): 438. https://doi.org/10.3390/gels8070438

[19] Wawrzkiewicz M, Hubicki Z. Removal of tartrazine from aqueous solutions by strongly basic polystyrene anion exchange resins. *J Hazard Mater.* 2009; 164: 502-509. https://doi.org/10.1016/j.jhazmat.2008.08.021

[20] Estefan E, Elystia S, Kuan WH, Sasmita A. Removal of methyl orange textile dye using magnetic chitosan microspheres adsorbent. *Water Pract Technol.* 2023; 18(12): 3280-3290. https://doi.org/10.2166/wpt.2023.201

[21] Pourreza N, Mirzajani R, Behbahani MT. Removal of brilliant cresyl blue from aqueous solutions using modified zirconia nanoparticles as an adsorbent under ultrasonic action. *Desalin Water Treat.* 2016; 57: 28999-9006. https://doi.org/10.1080/19443994.2016.1193060

[22] Kurniawati D, Sari TK, Adella F, Sy S. Effect of Contact Time Adsorption of Rhodamine B, Methyl Orange and Methylene Blue Colours on Langsat Shell with Batch Methods. 1st Int. Conf. Chem. Sci. Educ. (ICChSE), *J Phys Conf Ser.* 2021; 1788: 012008. https://doi.org/10.1088/1742-6596/1788/1/012008

[23] Wong S, AbdGhafar N, Ngadi N, Razmi FA, Inuwa IM, Mat R, Amin NS. Effective removal of anionic textile dyes using adsorbent synthesized from cofee waste. *Sci Rep.* 2020; 10: 2928. https://doi.org/10.1038/s41598-020-60021-6

[24] Freundlich H, Helle WJ. The Adsorption of cis- and trans-Azobenzene. *J Am Chem Soc.* 1939; 61(8): 2228-30. https://doi.org/10.1021/ja01877a071

[25] Langmuir I. The adsorption of gases on plane surfaces of glass. *J Am Chem Soc.* 1918; 40: 1361-402. https://doi.org/10.1021/ja02242a004

[26] Badri N, Zbair M, Sahibed-Dine A, Chhiti Y, Khamliche L, Bensitel M. Adsorption of Cationic Dyes by Waste Biomass Treated by Phosphoric Acid. *J Mater Environ Sci.* 2018; 9: 1636-1644. https://doi.org/10.26872/jmes.2018.9.6.182

[27] Janet A, Kumaresan R, Uma Maheswari S. Adsorption of Anionic and Cationic Dyes onto Granular Activated Carbon. *Middle-East J Sci Res.* 2015; 23(2): 308-17. https://doi.org/10.5829/idosi.mejsr.2015.23.02.22114

[28] Saha P, Chowdhury S. Insight into adsorption thermodynamics. *Thermodynamics*. 2011; 16: 349-64. https://doi.org/10.5772/13474

[29] Adheem HM, Jasim LS. Preparation and Characterization of a three-component hydrogel composite and study of kinetic and thermodynamic applications of adsorption of some positive and negative dyes from their aqueous solutions. 2nd Int. Sci. Conf. Al-Ayen Univ. IOP Conference Series: *IOP Conf Ser Mater Sci Eng*. 2020; 928: 052027. https://doi.org/10.1088/1757-899X/928/5/052027

[30] Mandal B, Ray SK. Removal of safranine T and brilliant cresyl blue dyes from water by carboxy methyl cellulose incorporated acrylic hydrogels: Isotherms, kinetics and thermodynamic study. *J Taiwan Inst Chem Eng.* 2016, 60: 313-327. https://doi.org/10.1016/j.jtice.2015.10.021

[31] Amara-Rekkab A. Efficient Removal of Brilliant Cresyl Blue from Solution Using *Inula racemosa*: Experimental Insights, DFT Modeling, and Docking Simulation. *Sep. Sci Technol.* 2024; 9(41): e202403331. https://doi.org/10.1002/slct.202403331

[32] Gong R, Li M, Yang C, Sun Y, Chen J. Removal of cationic dyes from aqueous solution by adsorption on peanut hull. *J Hazard. Mater.* 2005; 121(1-3):247-250. https://doi.org/10.1016/j.jhazmat.2005.01.029

[33] Hambisa AA, Regasa MB, Ejigu HG, & Senbeto CB. Adsorption studies of methyl orange dye removal from aqueous solution using Anchote peel-based agricultural waste adsorbent. *Appl Water Sci.* 2023; 13(24). https://doi.org/10.1007/s13201-022-01832-y

[34] Dakhil IH. Recycling of Agriculture Wastes for Efficient Removal of Methyl Orange Dye Using Batch Adsorption Unit. *IOP Conf. Ser.: Mater Sci Eng.* 2020; 881(1): 012186. https://doi.org/10.1088/1757-899X/881/1/012186

Ispitivanje efikasnosti prirodnog materijala za uklanjanje katjonskih oksazin- i anjonskih azo- boja iz vodenih rastvora

Asma Boudaoud[1], Chifaa Ad[2], Mebrouk Djedid[2], Mokhtar Benalia[2], Mounira Guermit[1] and Soltani Amel[3]

[1]Laboratory of Process Engineering, Materials and Environmental, Department of Common Trunk Science and Technology; Faculty of Technology, Amar Telidji University of Laghouat, Laghouat, Algeria
[2]Laboratory of Process Engineering, Materials and Environmental, Department of Process Engineering, Faculty of Technology, Amar Telidji University of Laghouat, Laghouat, Algeria
[3]Higher Normal School of Laghouat, Laghouat, Algeria

(Stručni rad)

Izvod

U ovom radu je ispitan procese adsorpcije boja brijant krezol plave (BCB) i metil narandžaste (MeO) na ljuske semena bundeve sa lokalnog područja (LPSH). LPSH adsorbent je analiziran primenom infracrvene spektroskopije sa Furijeovom transformacijom, skenirajuće electronske mikroskopije sa spektroskopijom rendgenskih zraka disperzivne energije, difrakcije rendgenskih zraka i Brunauer-Emmett-Teller analizom. Deskriptivnom analizom morfologije LPSH utvrđena je heterogena površina, dok je strukturnom analizom utvrđeno prisustvo funkcionalnih grupa tipičnih za lignocelulozne strukture. Potvrđena je mezoporozna površina adsorbenta, specifične površine ~1,53 m^2 g^{-1}. Studije izotermne adsorpcije sugerišu da je Langmuirov model najbolje opisao adsorpciju MeO, dok je Frojndlihov model pogodniji za opisivanje adsorpcije BCB. Prema termodinamičkim analizama, adsorpcija BCB je bila egzotermna i spontana, dok je adsorpcija MeO bila endotermna i nespontana. Rezultati procene efikasnosti LPSH adsorbenta su pokazali da su maksimalni kapaciteti adsorpcije ~81 mg g^{-1} za BCB boju i ~8,2 mg g^{-1} za MeO boju.

Ključne reči: Briljantna krezol plava; metil narandžasta; adsorpcija; ljuske semena bundeve; rastvori sintetičkih boja